Published in final edited form as:
Opt Lett. 2009 February 1; 34(3): 319–321.

Normalized Born ratio for fluorescence optical projection tomography

Claudio Vinegoni[1,*], **Daniel Razansky**[2], **Jose-Luiz Figueiredo**[1], **Matthias Nahrendorf**[1], **Vasilis Ntziachristos**[2], and **Ralph Weissleder**[1]

[1]Center for Systems Biology, Massachusetts General Hospital, Harvard Medical School, 185 Cambridge Street, Boston, Massachusetts 02114, USA

[2]Institute for Biological and Medical Imaging (IBMI), Technical University of Munich and Helmholtz Center Munich, Ingolstaedter Landstrasse 1, 85764 Neuherberg, Germany

Abstract

We present a normalized Born approach for fluorescence optical projection tomography that takes into account tissue absorption properties. This approach can be particularly useful to study fluorochrome distribution within tissue. We use the algorithm to three-dimensionally reconstruct and characterize a fluorescein isothiocyanate containing absorptive phantom and an infarcted mouse heart previously injected with a fluorescent molecular probe.

Optical projection tomography (OPT) [1] is a recently introduced three-dimensional imaging technique for primary use in developmental biology and gene expression studies [2]. Biological samples are typically rendered transparent by first dehydrating them and then placing them in a mixture of benzyl alcohol and benzyl benzoate (BABB or Murray's Clear solution) in a 2:1 ratio for several hours. Once cleared, the samples present very low scattering and absorption values, making their light diffusive contribution almost negligible. Fluorescence or absorption images of the samples are then taken over 360° angle projections with 1° or less steps [1]. The use of a lens with high telecentricity allows one to project photons that travel parallel to the optical axis of a CCD camera [3]. Because the scattering contribution is very low, absorption reconstructions are analogous to x-ray computed tomography and can be obtained using a common Radon backprojection algorithm.

In recent years we have seen a tremendous interest in the design of "smart" activatable optical agents designed to provide molecular information for *in vivo* imaging. These probes have been designed to work in the near-infrared to enable whole mouse imaging. Conversely it is equally important to image *ex vivo* whole (intact) organ probe distributions to determine molecular activity distribution with high resolution by using, for example, OPT. Unfortunately, the conventional clearing process can require several days, depending on the tissue of interest and can affect the quantum efficiency of the associated fluorochromes. To maximize sensitivity it is therefore necessary to shorten perfusion time, leading to a higher contribution in the absorption values. So far, fluorescence reconstructions have been obtained using an approach similar to absorption-based OPT [1]. However the varying spatially dependent absorption makes incorrect the use of the inverse Radon for backprojecting the fluorescence images, severely affecting the obtained fluorescent protein or fluorescent molecular probe distributions and quantification ability. Here we consider a problem of volumetric tomographic

*Corresponding author: cvinegoni@mgh.harvard.edu.

reconstruction of fluorescence emitted from a scattering-free absorbing object illuminated by a collimated source in a transillumination mode. In a discretized one-dimensional fashion, each ray at the excitation wavelength λ_{ex}, emitted from an arbitrary source position x_s, is exponentially attenuated as it passes through the imaged object. After exciting the fluorochrome located at position x, the radiation at the emission wavelength λ_{fl} is filtered and collected by the CCD's pixel located at position x_d using a telecentric lensing system. Although the emitted fluorescence does not follow the same path as the excitation ray, the intensity recorded at each pixel approximates a projection of all the fluorochromes excited along the entire focal zone corresponding to this particular excitation ray due to the system's high telecentricity. For fluorescence tomographic reconstructions, the imaged object is rotated 360° and multiple source-detector measurements $U_{ex}(x_s, x_d)$ and $U_{fl}(x_s, x_d)$ are acquired with the CCD camera at both λ_{ex} and λ_{fl}, respectively. These are then combined under the normalized Born (*n*Born) field $U_B(x_s, x_d)$ [4], i.e.,

$$U_B(x_s, x_d) = \frac{U_{fl}(x_s, x_d)}{U_{ex}(x_s, x_d)}. \quad (1)$$

The inversion problem, i.e., reconstruction of the fluorochrome distribution, can be facilitated by writing the forward model for both excitation and emission light propagation. The Green's function describing the excitation ray propagation follows a simple Beer-Lambert type attenuation through the absorbing object, i.e.,

$$G_{ex}(x_s, x) = e^{-\int_{x_s}^{x} \mu_a(x)\mathrm{d}x}. \quad (2)$$

The light intensity emitted from the source at position x_s and measured by the detector at position x_d on the CCD can be written as $U_{ex}(x_s,x_d)=B\cdot G_{ex}(x_s,x_d)$, where B incorporates all the experimental system-dependent constants. After collecting the object transillumination images $U_{ex}(x_s,x_d)$ at multiple projections, volumetric reconstruction of optical absorption coefficient $\mu_a(\vec{r})$ can be obtained as in regular OPT, i.e., using a filtered backprojection of Eq. (2). The precise distribution of the excitation light intensity $G_{ex}(x_s,x)$ along each ray path can then be calculated; $U_{fl}(x_s,x_d)$, the fluorescence intensity detected at detector x_d and stimulated by the light emitted from source x_s, comprises an added contribution of all the fluorochromes excited along the ray path, i.e.,

$$U_{fl}(x_s, x_d) = D\int_{x_s}^{x_d} G_{ex}(x_s, x)A(x)G_{fl}(x, x_d)\mathrm{d}x, \quad (3)$$

where $A(x)$ represents the fluorochrome absorption at position x and can generally be represented as $A = \varepsilon\eta C$, where ε, η, and C are the extinction coefficient, quantum yield, and concentration of the fluorophore, respectively. The parameter D represents the experimental system-dependent constants (we assume for both λ_{ex} and λ_{fl} similar tissue absorption, i.e., G_{fl} can be replaced with G_{ex}). The forward model of our imaging problem can then be written as

$$U_B(x_s, x_d) = \frac{\alpha}{G_{ex}(x_s, x_d)}\int_{x_s}^{x_d} G_{ex}(x_s, x)A(x)G_{ex}(x, x_d)\mathrm{d}x, \quad (4)$$

where α incorporates unknown constants associated with wavelength-dependent gains and attenuations that can be measured once for every imaging system. Finally, for the fluorescence reconstruction, the volume of interest is segmented into voxel elements and Eq. (4) is

discretized on the assumed mesh, i.e., $U_i = \Sigma_j W_{ij} A_j$, where W_{ij} are the "weight functions" that connect the measurements U_i to the unknowns A_j for each voxel j. The unknown voxel values A_j of the reconstructed three-dimensional image are found by inverting W_{ij}. It should be noted that, owing to negligible scattering, the forward model matrix here is much better conditioned as opposed to diffusion-based optical tomographies applied to heavily scattering objects. This is due to an accurate knowledge of the optical absorption distribution in the object [i.e., the Green's functions $G_{ex}(x_s, x_d)$, $G_{ex}(x_s, x)$, and $G_{ex}(x, x_d)$] from the preceding reconstruction obtained using regular absorption-based OPT.

The experimental setup described in this Letter is shown in detail in Fig. 1. The light sources are filtered with narrowband pass interference filters. The sample is immersed in a BABB solution and is held in place on a holder and rotated along its vertical axis. The fluorescein isothiocyanate (FITC) fluorescence signal and the far-red fluorescence signal are filtered through narrowband-pass interference filters coupled with their respective long-pass filters. The transillumination signal is detected by a CCD camera and images are acquired over 360 projections with 1° steps. To assess algorithm accuracy we built a cylindrical phantom that consists of two separate cylinders of 0.8% agarose gel fused together along their vertical axis. The bottom cylinder was fabricated by diluting a low concentration of India ink in the agarose gel to induce absorption while the top cylinder was left transparent. A hole was bored into the final fused cylinder along its vertical axis and filled with 1.5% agarose gel in which FITC dextrane was diluted to reach a 1 μM concentration. FITC dextran was used to prevent diffusion of the dye molecules into the surrounding agare. Figure 1(b) shows a diagram of the phantom and its geometry; fluorescence Fig. 1(c) and transmission images Fig. 1(d) are shown for the cleared phantom. To become imaged the sample was immersed in the BABB solution and 360 projections were obtained in both fluorescence and absorption mode. Reconstructions of planes for both attenuation coefficient and emission distribution were obtained. Figure 2(a) shows the reconstruction at level 1, where no absorption is present (upper figure) and at level 2, where India ink is present (lower figure). The clear inner circle present in the reconstruction is a section of the inner cylinder, where only dye (and not ink) is present. The fluorescence reconstruction of the phantom at the same levels (1 and 2) is shown in Fig. 2(b). While the inner cylinder contains a uniform concentration of dye for its entire length resulting in a 1:1 ratio in fluorochrome concentration, the fluorescence signal in the reconstructions is clearly lower for the plane in the absorptive agare (lower figure) and fails to report the 1:1 ratio in fluorochrome concentration. The normalized Born reconstruction [Fig. 2(c)] shows that the two reconstructions are similar (1:1 ratio). Fluorescence intensity plots taken at half circle are given before [Fig. 2(d)] and after [Fig. 2(e)] normalization. As evidenced from Figs. 2(c) and 2(e) the method is therefore valid and guarantees an accurate measurement of the relative fluorophores concentration. We then decided to apply our method for the fluorescence imaging of a mouse heart that had previously sustained a controlled infarct. The mouse was injected with Prosense-680, an activatable fluorescence sensor reporting on cathepsin activity in healing myocardium. This is a case of particular interest, because it could allow one to gain insight into the probe distribution within the heart and to study inflammatory responses after myocardial infarction. The heart was fixed and embedded in a 0.8% agarose gel, dehydrated, and cleared by immersion in a 2:1 BABB solution. A reconstruction of a single plane of the heart is shown in both absorption [Fig. 3(b)] and fluorescence [Fig. 3(c)]. The normalized Born reconstruction is presented in Fig. 3(d), and it shows the difference in the dye distribution within the heart after normalization.

In conclusion, we have presented a Born normalized approach for fluorescence OPT using a normalized transillumination approach. The weighted method was found to improve quantification performance over conventional OPT with samples that present nonnegligible values of absorption, as is the case for most tissue. This was demonstrated in both phantom and whole organ imaging experiments. The proposed approach provides the essential tools for

determining the correct fluorophores or fluorescent protein distribution in fluorescence OPT reconstructions and opens possibilities to extend OPT to new molecular imaging applications.

Acknowledgments

C. Vinegoni acknowledges support from National Institutes of Health (NIH) grant 1-RO1-EB006432.

References

1. Sharpe J, Ahlgren U, Perry P, Hill B, Ross A, Hecksher-Sorensen J, Baldock R, Davidson D. Science 2002;296:541. [PubMed: 11964482]
2. Lee K, Avondo J, Morrison H, Blot L, Stark M, Sharpe J, Bangham A, Coen E. Plant Cell 2006;18:2145. [PubMed: 16905654]
3. Oldham M, Sakhalkar H, Wang YM, Guo PY, Oliver T, Bentley R, Vujaskovic Z, Dewhirst M. J. Biomed. Opt 2007;12:1.
4. Ntziachristos V, Weissleder R. Opt. Lett 2001;26:893. [PubMed: 18040483]

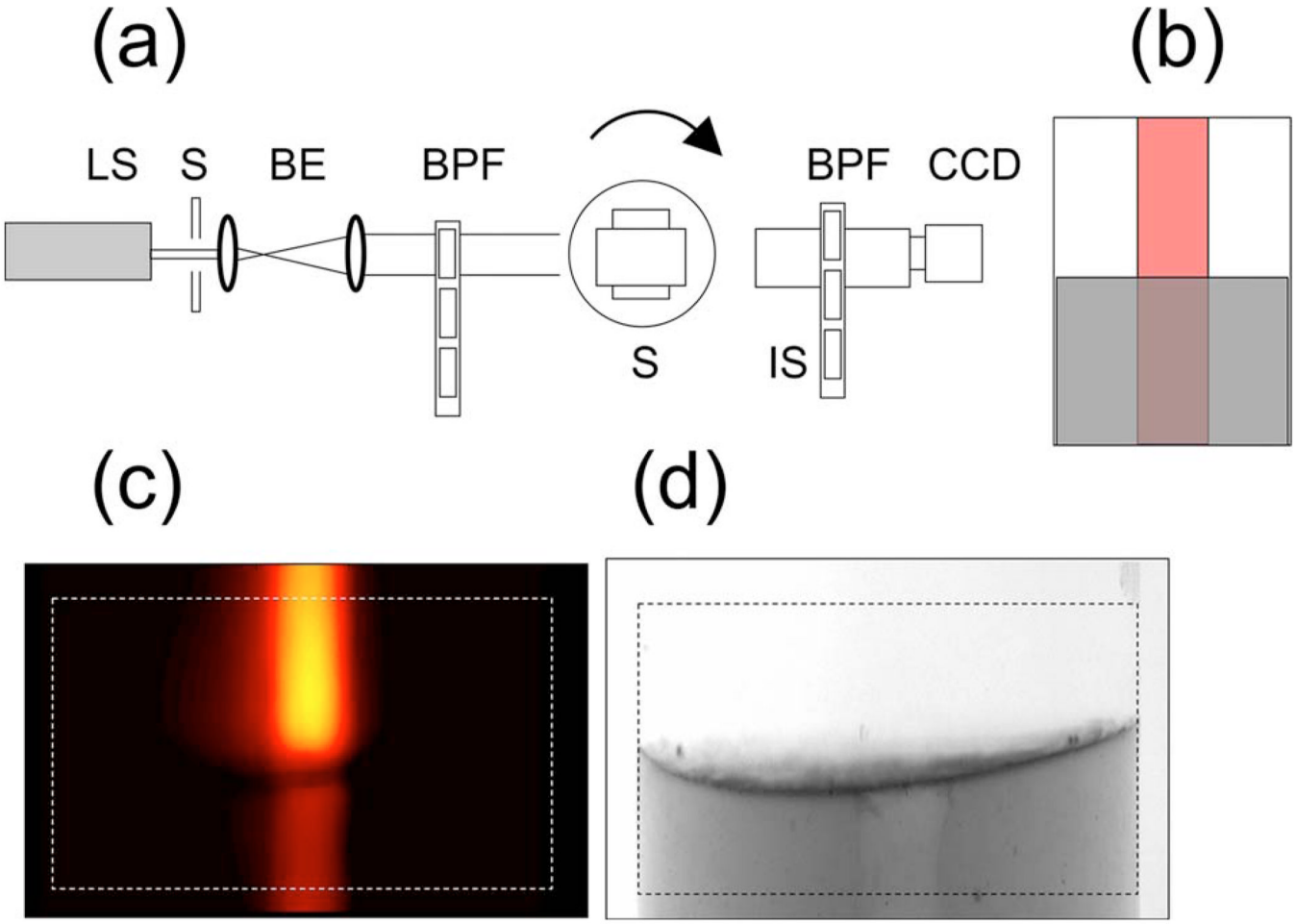

Fig. 1.

(Color online) (a) Experimental setup. LS, light source; S, shutter; BE, beam expander; BPF, filters; S, sample; IS, imaging system. (b) Schematic of the gel agarose phantom. The phantom consists of two separate cylinders fused together along their vertical axis, with the bottom one containing India ink (10 ppm). A hole is bored into the final fused cylinder along its vertical axis and filled with a 1 μM concentration of FITC dextran. (c) Phantom's fluorescence and (d) absorption projections.

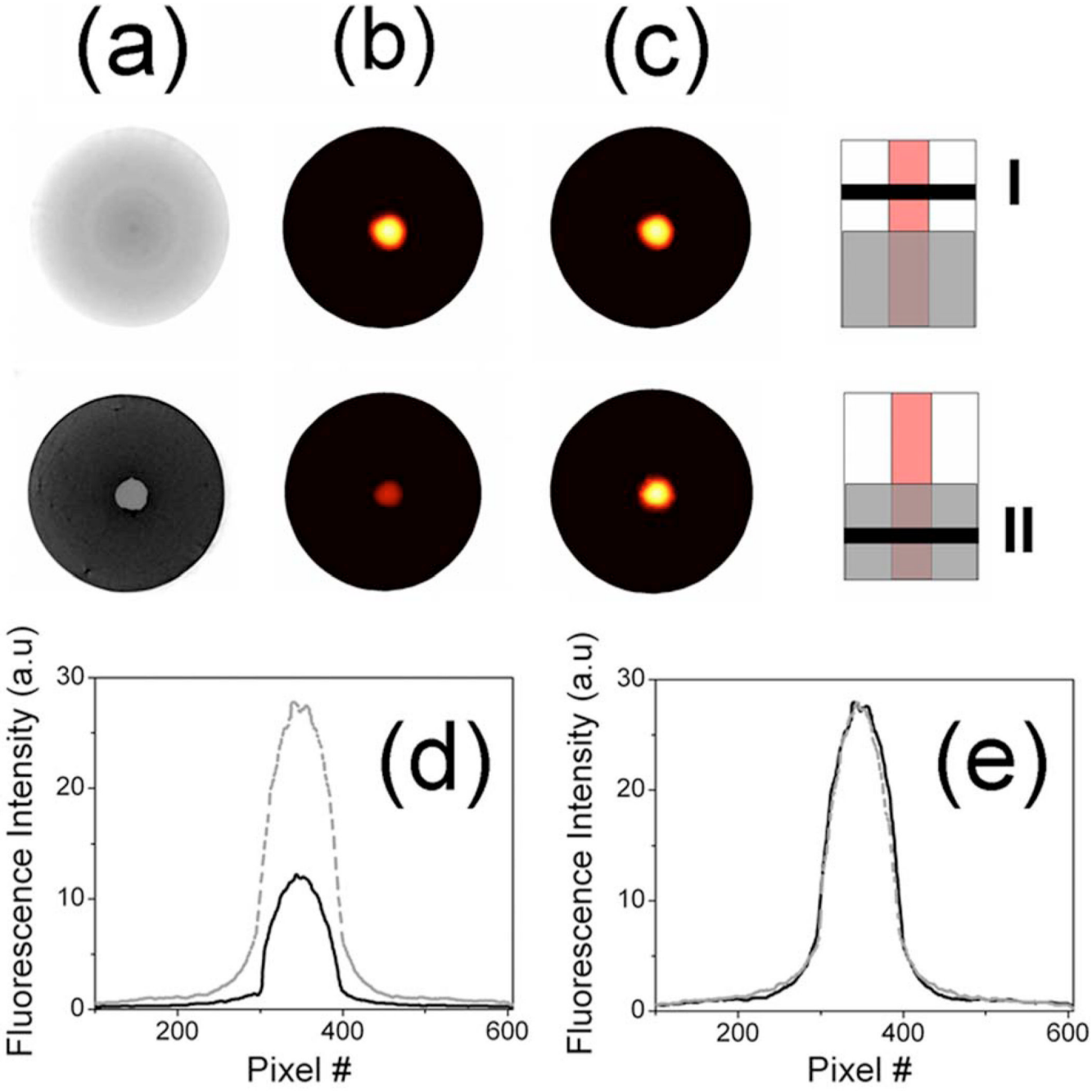

Fig. 2.

(Color online) Reconstructions at two different positions (I and II) along the phantom vertical axis. (a) Absorption (b) plain fluorescence, and (c) normalized Born reconstructions. (d) and (e) Fluorescence intensity plots along the reconstructions' center at level I and II are shown in dashed gray and continuous black, respectively. (d) Without and (e) with normalization correction.

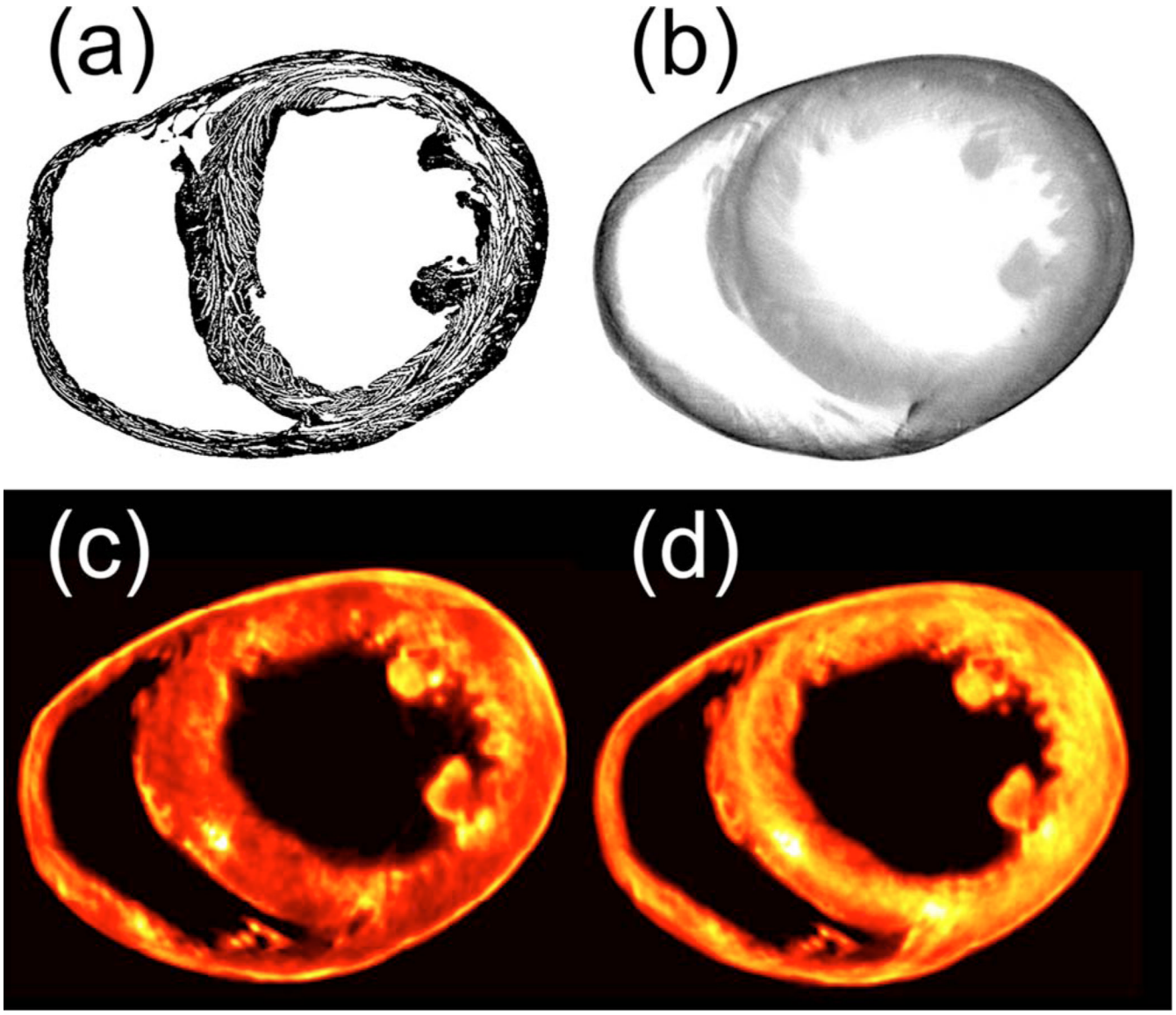

Fig. 3.
(Color online) Reconstructions of a mouse heart that had previously sustained a controlled infarct and was injected with Prosense-680. (a) Histology, (b) absorption reconstruction, (c) plain fluorescence reconstruction, and (d) normalized Born fluorescence reconstruction. The distribution of the fluorescent probe in (d) has been confirmed by correlative immunohistochemistry.